Collisional-radiative and average-ion hybrid models for atomic processes in high-Z plasmas

M. Itoh and T. Yabe
Institute of Laser Engineering, Osaka University, Yamada-oka, Suita, Osaka 565, Japan

S. Kiyokawa
Department of Physics, Nara Women's University, Kitauoyanishi-cho, Nara 630, Japan
(Received 30 January 1986; revised manuscript received 28 July 1986)

A new time-dependent atomic model is presented. In the model, called the hybrid-atom model (HAM), the energy-functional form of the population probability obtained from the average-ion model is used to estimate the level population of ions having charge different from the average ion. In medium-Z plasmas HAM gives results similar to the collisional-radiative (CR) model. The required computation time is comparable to the average-ion model even for high-Z plasmas. In these plasmas the CR model becomes impracticable. Though the model partly uses the average-ion model, the x-ray emission calculated is significantly different.

I. INTRODUCTION

Experiments have shown that there are high rates of x-ray emission from hot and dense high-Z plasmas produced by laser interaction. Therefore, an accurate calculation of the emission rate from laser-produced high-Z plasmas is indispensable. The ranges of electron density from 10^{19} to 10^{24} cm^{-3} and temperature from 100 eV to a few keV in these plasmas are such that neither local-thermodynamical-equilibrium (LTE) nor coronal-equilibrium (CE) can be used over the entire domain. In such non-LTE cases, the population $N_{z,n}$ of each ion charge state z in the nth level is generally required to calculate x-ray emission from the plasma.[1,2] For a high-Z plasma, the equation for this population is rarely solved. Consequently, in analyzing radiation from a laser-irradiated high-Z target, the average-ion model[3–8] has been widely used. This is mainly because the model requires fewer rates to be calculated thereby consuming less computation time and hence can be coupled into any hydrodynamic code. In the average-ion model, $N_{z,n}$ is averaged over z and it is sufficient to solve only the equations for the level populations of an average atom. As an alternative approach, if a suitable assumption for the population of the excited-level populations can be made, the equations required to be solved are those for N_z only; N_z being the abundance of the ion z. In this direction, Salzmann and Krumbein[9] proposed a form of the excited-level population such as $N_{z,n}/N_z = N_0 A \exp(-E_{z,n}/kT)$ for excited levels and $N_{z,n}/N_z = N_0$ for a ground level where A is so chosen that the population becomes close to the value calculated by a detailed rate equation. Here, N_0 is determined from $\sum_n N_{z,n}/N_z = 1$ and $E_{z,n}$ is the level energy. However, this is not always possible for high-Z plasmas, since we have no method to determine the adjustable parameter A. Busquet[10] proposed a mixed model where only relatively lower excited levels are calculated by the rate equation whereas highly excited levels are assumed to be of the Boltzmann type. However, he needed a further approximation in the coronal limit.

In this paper, we report that the excited-level populations for ions in different charge states have a common characteristic and propose to use the average-ion model to characterize this common behavior. This enables us to calculate both the level populations and the charge-state distribution even for high-Z materials with computation time comparable to the average-ion model. Since this model uses a combination of the collisional-radiative model and the average-ion model, we refer to it as the "hybrid-atom model" (hereafter, HAM).

In Sec. II, the average-ion model used is briefly reviewed and then we describe the detailed procedure and the concept of HAM in Sec. III. The atomic processes and the corresponding formulas for rate coefficients are discussed in Sec. IV. In Sec. V, we show some examples which clarify the essential advantages of HAM over the average-ion model by analyzing the x-ray emission from high-Z plasmas.

II. THE AVERAGE-ION MODEL

In general, the rate equation for the population $N_{z,n}$ of an ion in charge state z with an excited electron in the nth level is

$$\begin{aligned} dN_{z,n}/dt = &-\sum_m I_{z,n;z+1,m} N_{z,n} N_e - \sum_k R_{z,n;z-1,k} N_{z,n} N_e + \sum_{m'} I_{z-1,m';z,n} N_{z-1,m'} N_e + \sum_{k'} R_{z+1,k';z,n} N_{z+1,k'} N_e \\ &- \sum_l E_{z,n;z,l} N_{z,n} N_e - \sum_s D_{z,n;z,s} N_{z,n} + \sum_s E_{z,s;z,n} N_{z,s} N_e + \sum_l D_{z,l;z,n} N_{z,l} , \end{aligned} \tag{1}$$

where $z=0,1,2,\ldots,z_0$ (z_0 is the nuclear charge) and $n=1,2,\ldots,n_{\max}$. Here I, R, E, and D are the rate coefficients for ionization, recombination, excitation, and deexcitation, respectively. The subscripts indicate the charge state and the level number of initial and final states.

In the average-ion model, Eq.(1) is statistically treated and modified into the equation for an average ion with $z=z^a$. According to the procedure described in Appendix B, Eq. (1) is modified to be

$$d(NP_n)/dt=R_nN_eNQ_n-I_nN_eNP_n+N\left[\sum_{m>n}A_{nm}P_mQ_n-\sum_{m'<n}A_{m'n}P_nQ_{m'}\right]+\sum_{m>n}C^D_{nm}N_eNP_mQ_n$$
$$-\sum_{m'<n}C^D_{m'n}N_eNP_nQ_{m'}+\sum_{m<n}C^U_{nm}N_eNP_mQ_n-\sum_{m'>n}C^U_{m'n}N_eNP_nQ_{m'}\ ,\quad Q_n=1-P_n/g_n \tag{2}$$

where Q_n is the fractional vacancy, N and N_e are the ion number density and free-electron number density, respectively, and g_n is the statistical weight of the electron in the nth level. It should be noted that P_n is the fractional number of electrons in the nth level and is not a probability to find an electron ($\sum_n P_n\neq 1$) in the nth level. Here R_n, I_n, A_{nm}, C^D_{nm}, and C^U_{nm} are the rate coefficients for recombination into the nth level, ionization from the nth level, Einstein's A coefficient, collisional deexcitation (from m to n), and collisional excitation (from m to n), respectively. The recombination rate R_n consists of the radiative, three-body, and dielectronic recombinations. The free-electron number density N_e is related to an average ion charge z^a as

$$N_e=Nz^a=N\left[z_0-\sum_n P_n\right]\ . \tag{3}$$

The energy of bound electrons E_n is given by

$$|E_n|=13.6q_n^2/n^2-\Delta E_n\ (\text{eV}) \tag{4}$$

where q_n is the effective nuclear charge, e.g., the net nuclear charge as seen by an electron in the nth level, which is calculated with Mayer's screening constants σ_{nm} as $q_n=z_0-\sum_m\sigma_{nm}P_m$.[5,7,11] The subscript z on $E_{z,n}$ will be omitted hereafter for the average ion $z=z^a$ without introducing any ambiguity. ΔE expresses a potential lowering by perturbers such as free electrons and neighboring ions. The pressure ionization effect is added to the calculation by forcing the degeneracy of the nth bound-electron shell to decrease to zero at a high-density limit: the electron populations around the valence shell ($r_n\simeq R_0$) are numerically modified so that the solution is close to the Thomas-Fermi description in the high-density region. Here r_n and R_0 are the electron-orbital radius and ion-sphere radius, respectively.[7]

III. HYBRID ATOM MODEL

It is very difficult to determine the electron population in each level of every ion, particularly for high-Z materials such as Au. Since some ions that give the major contribution to the emission from the plasma are in a charge state close to the average ion, it is sufficient to determine the electron population for ions having z close to z^a without accurately calculating the electron population for every ion. For $z\simeq z^a$, the electron population in each level is expected to have a similar characteristic to that of the average ion.

If the level populations of the excited states are known, Eq. (1) can be reduced to

$$dN_z/dt=-I_zN_zN_e-R_zN_zN_e+I_{z-1}N_{z-1}N_e$$
$$+R_{z+1}N_{z+1}N_e\ , \tag{5}$$

where I_z and R_z are the respective rate coefficients summed over all excited states, and are defined in Sec. IV.

Then, how are we to determine the level population of the excited states? We propose to employ the average-ion model. The basic principle of our approximation comes from the fact that transitions between bound states proceed faster than those between free and bound states. Hence, the level populations of the excited levels can be approximately estimated by quasisteady equations of bound-bound transitions for an ion of charge z:

$$N_{z,n}/N_{z,m}\simeq(A_{nm}+C^D_{nm}N_e)/(C^U_{mn}N_e)$$
$$=(g_n/g_m)F(E_m,E_n,N_e)\ , \tag{6}$$

The last expression of F is easily seen from Eqs. (16), (17), and (18) in Sec. IV. Equation (6) shows that the normalized population $N_{z,n}/g_n$ can be estimated if only the level energy E_n is known. Although there exist transition processes other than those used in Eq. (6), Eq. (6) motivates us to use an energy-functional form of the normalized population $N_{z,n}/g_n$: if $N_{z,n}/g_n$ is only a function of level energies and does not depend explicitly on z, the normalized populations constructed from the average ion can be rescaled and used for other ions in a different charge state z.

In order to clarify the idea further in detail, let us examine the level dynamics of various ions by solving the full rate equation (1) for an aluminum plasma. Here we used the collisional-radiative model similar to that of

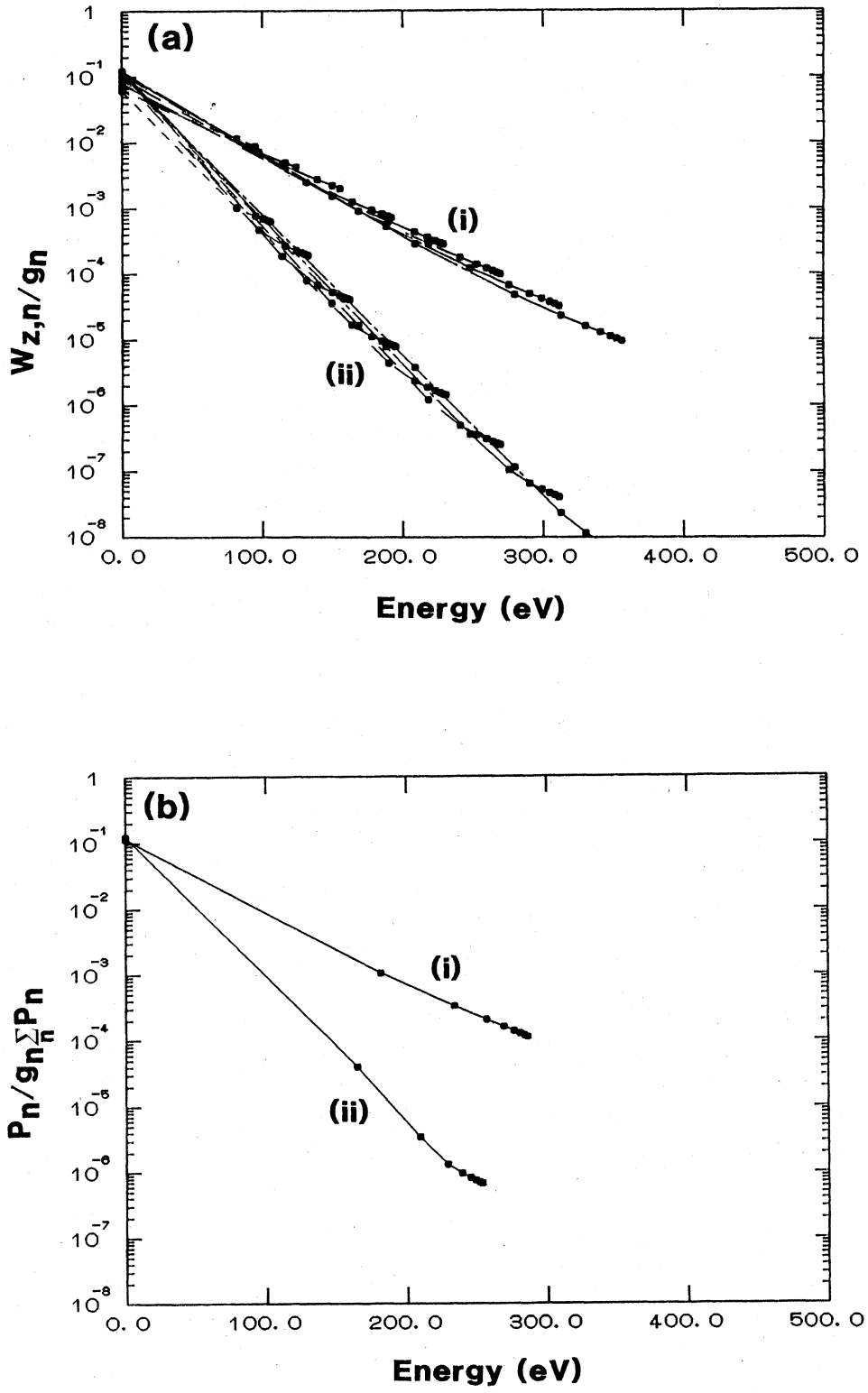

FIG. 1. The reduced population probability vs the excitation energy for $T_e = 50$ eV and (i) $n_i = 10^{20}$ cm^{-3} and (ii) $n_i = 10^{18}$ cm^{-3}. (a) The reduced ion population probability vs the excitation energy with CR model for different charge states of ions. (b) The reduced electron population probability versus the excitation energy with the average-ion model.

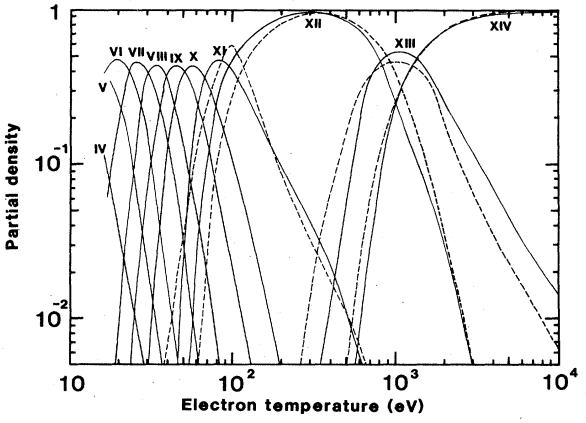

FIG. 2. The dependence of aluminum abundance in various charge states on electron temperature for an ion density of 10^{20} cm^{-3}. The solid and dashed lines are the results from the hybrid-atom model and the collisional-radiative model, respectively.

Colombant *et al.*[1] In Fig. 1(a), the reduced population probability $W_{z,n}/g_n$ $(=N_{z,n}/g_n N_z \sum_n W_{z,n}=1)$ is plotted versus the excitation energy, which means the level energy measured from the ground-state level. For $N_i=10^{20}$ cm^{-3}, the probability is close to the Boltzmann type $W_{z,n}\sim g_n \exp(-E_n/kT_e)$. Although for $N_i=10^{18}$ cm^{-3} it is also close to the Boltzmann type, the temperature of the bound electrons is much lower than the free electron temperature T_e. In each case, the reduced probability for various ions of $+3$ to $+10$ can be well characterized universally by one curve, although this curve depends on the physical parameters as shown by the two curves in Fig. 1(a).

If this characteristic is taken into account, the common behavior appearing in Fig. 1(a) can be satisfactorily described by the average-ion model. Actually, the reduced electron population probability defined later shows the same characteristics as shown in Fig. 1(b). Accordingly, once the electron population P_n of the average ion is obtained by Eq. (2), the function $Y_a(E)$ (the reduced electron-population probability) is constructed from P_n as follows; at some discrete points

$$Y_a(E_n^a)=P_n/g_n\sum_n P_n \quad (n=1,2,\ldots,n_{\max}) \tag{7}$$

and in other regions Y_a(E) is exponentially interpolated from Eq. (7): this exponential interpolation is justified by the characteristics appearing in Fig. 1. In Eq. (7) E_n^a is the excitation energy of the average ion and the summation is taken over the ionizing shells. This energy-functional form can be used to generate the population probability even for the ion in a charge state z different from z^a of the average ion:

$$W'_{z,n}=Y_a(E)g_n \ . \tag{8}$$

It should be noticed that the physical meaning of $W'_{z,n}$ in Eq. (8) differs from $W_{z,n}$ in Fig. 1(a): the former is derived from the electron population but the latter from the ion population $N_{z,n}$. However, both characteristics are similar as seen from Figs. 1(a) and 1(b). This can be justified by remembering the nature of the average ion model and CR model. In the CR model, only one electron is excited in some level. Accordingly, if ions in various charge states are collected together into a fictitious ion, the electron population P_n in the nth level of this ion will be similar to the ion population of the original "real" ions $N_{z,n}$ with an electron in the nth level.

In the next step, the ionization and recombination rate coefficients are summed up with respect to n using N_z and $W_{z,n}=W'_{z,n}$. Then Eq. (5) for N_z is solved. With this model, all regions including LTE, corona, and those intermediate to them can be described without any adjustable parameter.

In addition to the characteristics shown in Fig. 1, the average-ion model has many advantages in constructing the energy-functional form [Eq.(7)]. These are (1) if N_z peaks at $z=z^a$, it is enough for the common characteristics as in Fig. 1 to be valid only for z close to z^a, (2) even if z^a changes in time, the average ion can follow this z^a and hence the charge state of primary interest can be satisfactorily traced, and (3) the number of equations to be solved is $z_0+n_{\max}$ instead of $z_0 n_{\max}$ in the full rate equations.

Since Eq. (5) has a tridiagonal form, the numerical procedure to solve it is quite easy. In the present model the main computation time becomes the time to solve only Eq. (2) and is computationally as fast as the average-ion model. If the ionic charge becomes large, then the validity of the present model is much improved because the range of z that satisfies $\epsilon=|z-z^a|/z^a \ll 1$ becomes wider and the fractional energy change $(\Delta E/E)$ for these ions is on the order of ϵ; this small change of energy justifies the interpolation in constructing the energy function Y_a.

In order to justify the model, let us give an example. Figure 2 shows the relative abundance of the charge state of aluminum at a steady state for $N_i=10^{20}$ cm^{-3} and various electron temperatures. Here, the rate equation [Eq. (5)] for N_z includes radiative, three-body, and dielectronic recombinations, and collisional ionization. In addition, collisional excitations and deexcitations, and radiative deexcitations, are also included in the average-ion model [Eq. (2)]. The results predicted by the hybrid-atom model [Eqs. (2) and (5)] (solid line) agree quite well with those given by Duston *et al.*[2] (CR model shown by the dashed line) for $z\geq 10$. In Ref.2 only levels for $z\geq 10$ were calculated by the rate equation, whereas for $z<10$ ions only the ground-state levels were taken into account. The small difference (about 40% at most) between the CR model and our hybrid-atom model is within differences caused by the different rate coefficients.

IV. ATOMIC PROCESSES

The collisional and radiative processes which are included in the present model are given in this section.

A. Collisional ionization

In hot plasmas there are two major ionizing processes, namely, collisional ionization by electron impact and photoionization by the radiation field. We can neglect the latter, for an optically thin plasma. For an optically thick

TABLE I. Values of C, ζ, and $F(u)$ from various authors.

Author	C ($\mathrm{cm}^{-3}/\mathrm{eV}^{3/2}\,\mathrm{sec}$)	ζ	$F(u)$
Landshoff-Perez	1.24×10^{-6}	2	$0.915(1+0.64/u)^{-2}+0.42(1+0.5/u)^{-2}$
Lotz	3×10^{-6}	1	$\mathrm{Ei}(u)\exp(u)$
Seaton	2.15×10^{-6}	2	1
McWhirter	2.34×10^{-7}	$\frac{7}{4}$	1

plasma, the radiation field must be treated together with the atomic processes as will be discussed in the next section and in Appendix A.

Although there is still no universally accepted expression for the collisional-ionization rate coefficient, one can find several formulas in the literature. These are due to Landshoff and Perez,[12] Lotz,[13] Seaton,[14] and McWhirter.[15] All these formulas have the same following form:

$$I_{z,n}=CT^{-3/2}[\exp(-u)/u^{\xi}]F(u)\ ,\qquad u=E_{z,n}/T\ , \tag{9}$$

where C is a numerical coefficient, T is the electron temperature in eV, and $F(u)$ is a function peculiar to the various formulas. In Table I, we list C, ζ, and $F(u)$ corresponding to the various approximations. $E_{z,n}$ is the level energy including the lowering of the ionization potential.

This formula is used both in Eqs. (2) and (5). When Eq. (9) is substituted into Eq. (5), the ionization rate coefficient must be summed up with respect to n using $W_{z,n}$:

$$I_z=\sum_n I_{z,n}W_{z,n}\xi_n\ , \tag{10}$$

where ξ_n is the number of electrons in the ionizing shell.

B. Three-body recombination

Three-body recombination is the inverse process to collisional ionization. From a detailed balancing consideration one obtains

$$R^{3\text{-}b}_{z,n}=1.66\times10^{-22}T^{-3/2}N_e g_{z,n}\exp(u)\times I_{z-1,n}\ \mathrm{cm}^3\,\mathrm{sec}^{-1}\ . \tag{11}$$

This becomes a dominant process as the density increases, resulting in thermodynamic equilibrium.

C. Radiative recombination

For hydrogenic ions the rate of radiative recombination is given by[16]

$$R^{r}_{z,n}=5.20\times10^{-14}q_{z,n}u^{3/2}\exp(u)E_i(u)\ \mathrm{cm}^3\,\mathrm{sec}^{-1}\ , \tag{12}$$

where $q_{z,n}$ is the effective nuclear charge and E_i is the first exponential integral and can be approximated as

$$\exp(x)E_i(x)=\begin{cases}\exp(x)(-\ln(x)-0.577\,215\,66+x) & \text{for } x\le10^{-4}\\ \exp(x)[-\ln(x)-0.577\,215\,66+0.999\,991\,93x-0.249\,910\,55x^2 & \\ \quad+0.055\,199\,68x^3-0.009\,760\,04x^4+0.001\,078\,57x^5] & \text{for } 10^{-4}<x\le1\\ \dfrac{x+2.334\,733+0.250\,621/x}{x^2+3.330\,657x+1.681\,534} & \text{for } +x>1\ .\end{cases}$$

D. Dielectronic recombination

The rate of dielectronic recombination introduced by Burgess[17] is in the form[6]

$$R^{d}_{z,n}=2.40\times10^{-9}B(q_{z,n})D(q_{z,n},T)T^{-3/2}\times\sum_m f_{mn}A(y)\exp(-E_{mn}/T)\ \mathrm{cm}^3\,\mathrm{sec}^{-1}\ , \tag{13}$$

where

$$B(q)=q^{1/2}(q+1)^{5/2}(q^2+13.4)^{-1/2}\ ,$$

$$E_{mn}=(E_{z,m}-E_{z,n})/a\ ,$$

$$a=1+0.015q^3/(q+1)^2\ ,$$

$$y=(q+1)(n^{-2}-m^{-2})\ ,$$

$$A(y)=0.5y^{1/2}/(1+0.210y+0.030y^2)\ ,$$

$$D(q,T)=0.0015[(q+1)n_t]^2/\{1+0.0015[(q+1)n_t]^2\}\ ,$$

and

$$n_t=1.508\times10^{17}q^6T^{1/2}/N_e\ .$$

From the above three expressions, the total recombination rate is

$$R_{z,n}=R^{3\text{-}b}_{z,n}+R^{r}_{z,n}+R^{d}_{z,n}\ . \tag{14}$$

Further, in order to use it in Eq. (5), it must be summed over n:

$$R_z=\sum_n R_{z,n}Q_{z,n}\ , \tag{15}$$

where the $Q_{z,n}$ is the fractional vacancy in the atomic shell.

E. Collisional excitation

In excitation as well as in ionization, there are two major processes: Collisional and radiative processes. The photoexcitation will be discussed in detail in the next section and in Appendix A. The collisional excitation rate can be written in the form[14]

$$C^U_{mn}=1.58\times10^{-5}f_{mn}T^{-1/2}E^{-1}_{mn}\exp(-E_{mn}/T)G_{mn} \quad \mathrm{cm^3\,sec^{-1}}, \tag{16}$$

$$E_{mn}=E_n-E_m ,$$

where f_{mn} is the oscillator strength for the $n\rightarrow m$ transition ($n>m$), E_{mn} is the excitation energy in eV and G_{mn} is the Gaunt factor.

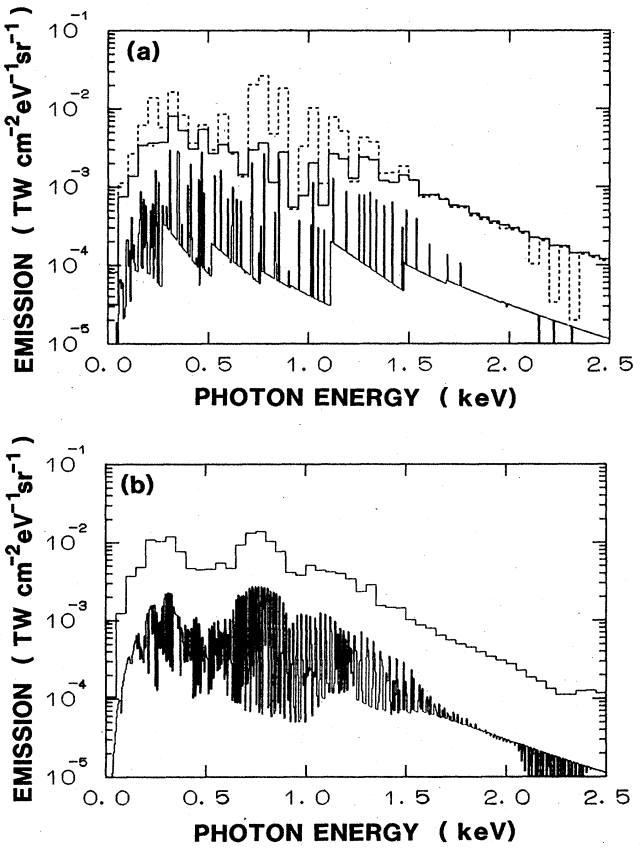

FIG. 3. The emitted x-ray intensity vs photon energy from a typical laser-produced Au plasma in which for simplicity the density and temperature are approximated by exponential functions in space balancing pressure: the range from 16×10^{20} cm^{-3}, 100 eV to 1×10^{20} cm^{-3}, 1600 eV, the scale length being 10 μm. (a) The results with the average-ion model. The solid lines are the results in which the energy space was divided into groups of 5 eV width: the lower curve is the direct data and the other is further averaged over 50 eV only in the final result, the former is drawn being reduced in its magnitude by a factor of 10. The dashed line is the result with the groups of 50 eV width broadened artificially during the ray trace calculation. (b) The results with the hybrid-atom model. The lower line indicates those calculated by the energy space divided into groups of 5 eV width, and another line indicates those further averaged over 50 eV only in the final result after the ray trace calculation.

F. Collisional deexcitation

The rate of collisional deexcitation is obtained from a detailed balance of the collisional excitation rate:

$$C^D_{nm}=(g_n/g_m)\exp(E_{mn}/T)C^U_{mn} . \tag{17}$$

G. Radiative decay

The rate of radiative decay ($m\rightarrow n$) is determined by the Einstein coefficient for spontaneous emission:

$$A_{nm}=4.315\times10^7(g_n/g_m)f_{mn}(E_{mn})^2\ \mathrm{sec^{-1}} . \tag{18}$$

H. Oscillator strength and gaunt factor

In the case of the hydrogenlike ion, the oscillator strength and the Gaunt factor are given, respectively, in the forms[18,19]

$$f_{mn}=1.96\frac{q_n^4q_m^2}{n^5m^3}\left[\frac{q_n^2}{n^2}-\frac{q_m^2}{m^2}\right]^{-3} , \tag{19}$$

$$G_{mn}=0.19\left[1+0.9\left\{1+\frac{n(n-m)}{20}\times\left[1+\left[1-\frac{2}{z_0}\right]\chi_{mn}\right]\right\}\times\exp(\chi_{mn})E_i(\chi_{mn})\right] \tag{20}$$

where $\chi_{mn}=E_{mn}/T$.

The change in charge state of an ion [dN_z/dt; Eq. (5)] is calculated using the rate coefficients I_z [Eq. (10)] and R_z [Eq. (15)]. The properties of average ions are calculated with Eq. (2) with coefficients $I_{z,n}$ [Eq. (9)], $R_{z,n}$ [Eq. (14)], C^U_{mn} [Eq. (16)], C^D_{nm} [Eq. (17)], and A_{nm} [Eq. (18)].

V. APPLICATION TO LASER-PRODUCED HIGH-Z PLASMAS

In the previous sections, we proposed a new atomic model, HAM, which solves Eq. (5) by constructing the level population $N_{z,n}=W_{z,n}N_z$ from the electron population given by the average-ion model, Eq. (2). In this section, we apply HAM to laser-produced Au plasmas.

As a simple example of such plasmas, we use exponential profiles for the density and temperature in space making the pressure uniform: the density and temperature ranges from 16×10^{20} to 1×10^{20} cm^{-3} and 100 to 1600 eV. The scale length of these plasmas is 10 μm. Figures 3(a) and 3(b) are obtained from the average-ion model and the hybrid-atom model, respectively. In addition to the atomic processes given in the Secs. II–IV, photoexcitations and radiation transport are included here. The formalism of the latter two processes is given in the Appendix A. In Fig. 3, the solid lines are the results in which

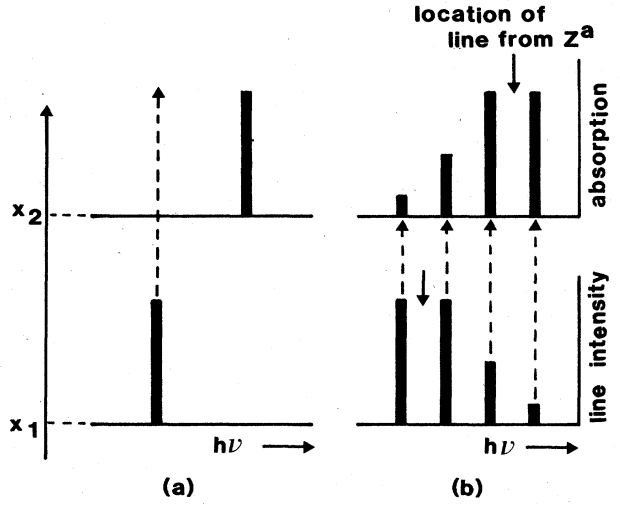

FIG. 4. It is schematically shown that the average-ion model is unsuitable for line transport. Let us imagine that the line radiation is emitted at some spatial point x_1 and absorbed at x_2. (a) In the average-ion model, there is only one fictitious ion at each space. The level energy of the ion changes from space to space depending on the average charge z^a which follows physical parameters. Consequently, the level energy shift between x_1 and x_2, which does not occur in actual plasmas, exists and the line radiation emitted at x_1 is no more absorbed by the same spectral line at x_2. (b) In HAM, there exists an ion having the same charge z in all regions although the abundance N_z changes from space to space. This means that a spectral line emitted at one region can always be absorbed by the same line in whole space. However, with varying amount.

the energy space was divided into groups of 5 eV width and line broadenings by various processes are neglected for simplicity: one line is the direct data and another is further averaged over 50 eV for an illustrative purpose. In Fig. 3(a), in addition to the above lines, we draw the dashed line that is the result using the groups of 50 eV width broadened artificially. The comparison between the solid lines in Figs. 3(a) and 3(b) shows that the emission intensities and hence the opacities with the hybrid-atom model are larger than those with the average-ion model. The difference is concluded to arise from the charge-state distribution.

In Fig. 4, this effect is schematically shown. Let us consider x-ray emission at some spatial point x_1 and absorption at x_2. In the average-ion model, only one fictitious ion having z^a exists at each space point, so that the level energy and hence the x-ray spectral energy changes from space point to space point depending on the average charge z^a which follows physical parameters, the density and the temperature. Consequently, the line radiation emitted in one region can not be absorbed by the same spectral line in another region as shown in Fig. 4(a). In actual plasmas, however, there exists an ion having the same charge z in all regions although the abundance N_z may change from space point to space point. This means that a spectral line emitted in one region is always absorbed by the same line in any other region of space as shown in Fig. 4(b). The hybrid-atom model can describe this process.

Figure 5 shows the fractional abundance of N_z for gold in the same regions as in Fig. 3: (a) the density 16×10^{20} cm^{-3}, the temperature 100 eV, (b) 8×10^{20} cm^{-3}, 200 eV, (c) 4×10^{20} cm^{-3}, 400 eV, (d) 2×10^{20} cm^{-3}, 800 eV, (e) 1×10^{20} cm^{-3}, 1600 eV. This distribution suggests that the line spectra is spread over a few hundred eV in spectral range because the energy difference between z and $z+1$ ions is about $2I_Hz/n^2$ and hence is about 50 eV for $z=30$ and $n=4$, I_H being 13.6 eV. If we examine the curves (d) and (e) in Fig. 5, the difference of charges at peak abundance [average ions of (d) and (e)] is 5 and this causes an energy difference of 300—400 eV ($n=4$) in the spectral lines. However, the spectral lines emitted by the ions from $+40$ to $+42$, for example, in the region (d) are surely absorbed by the same lines of ions from $+40$ to $+42$ in region (e).

It is interesting to see that the emitted spectra are close to those of the hybrid atom model as shown by the dashed line in Fig. 3(a), if the line opacity is averaged and smoothed over the energy group of 50 eV width during the ray trace calculation. This artificial broadening probably takes account of the spread of lines owing to the ion charge distribution.

It is worthwhile to note that the line integration in the radiative transfer equation, Eq. (A1), played an essential role in the obtained spectra in Fig. 3, and the contribution from the population change due to photoexcitation in Eq.(A8) was negligibly small in this particular example. We found, however, that this is not the case in the example given by Duston *et al.*[2]

VI. CONCLUSION

In summary, we propose a new atomic model, the hybrid-atom model, which takes advantage of the common characteristics in the level dynamics of excited states; these characteristics are justified by the full rate equation. Fortunately, this common nature was shown to be well characterized by the average-ion model. This information on the level population greatly simplifies the rate equation. In medium-Z plasmas, our model agrees well with the CR model. Even in high-Z plasmas, the model can

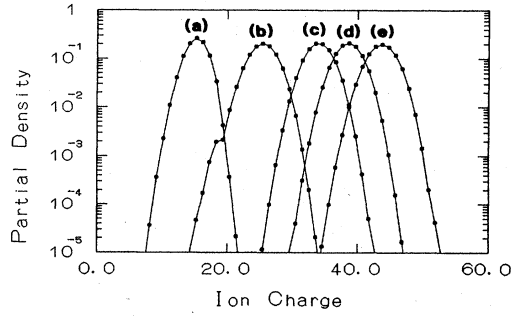

FIG. 5. The relative abundance of ions in various charge states calculated by the hybrid-atom model for (a) the density 16×10^{20} cm^{-3},the temperature 100 eV, (b) 8×10^{20} cm^{-3}, 200 eV, (c) 4×10^{20} cm^{-3}, 400 eV, (d) 2×10^{20} cm^{-3}, 800 eV, (e) 1×10^{20} cm^{-3}, 1600 eV.

calculate the level dynamics of ions as well as the charge-state distribution with a computation time only a few times longer than that for the average-ion model calculation.

The present model was also applied to x-ray emission from a laser-produced Au plasma. The existence of ions in the various charge states makes the line transport calculation more realistic. The comparison between the present model and the average-ion model shows that the latter underestimates the line opacity. The width of the ion charge distribution $\Delta Z \sim \pm 3$ obtained by the present model agrees with recent experimental implications.[20]

To conclude we point out subjects yet to be solved. One is the radiation transport: since a number of lines exist in high-Z plasmas, a simplified treatment of line transport will be a problem of the first priority. The second is the treatment of metastable states: forbidden transitions become important in high-Z plasmas.[21] These scale as z^8–z^{10}. The extension of the HAM to treat these processes is not straightforward. Some methods to separately incorporate forbidden transitions in the HAM may be necessary.

ACKNOWLEDGMENTS

The authors would like to thank Dr. B. Goel and Dr. R. Fröhlich at Kernforschungszentrum Karlsruhe GmbH, Dr. Y. Kitagawa at the Institute of Laser Engineering (ILE), Osaka University, Dr. T. Fujimoto at Kyoto University, Dr. T. Kato at the Institute of Plasma Physics, Nagoya University, and Professor C. Yamanaka at ILE, Osaka University for discussions and encouragement.

APPENDIX A

Here, we discuss photoexcitation processes and radiation transport in order to extend HAM to optically thick plasmas. The specific spectral intensity I_ν is calculated by the transfer equation

$$\frac{dI_\nu}{ds} = j_\nu - \kappa'_\nu I_\nu \ , \tag{A1}$$

where j_ν is the emission coefficient, κ'_ν the absorption rate including induced emission, ν the frequency, and s denotes the propagation distance of the radiation. For bound-bound transitions, j_ν is expressed as

$$j_\nu = \frac{h\nu}{4\pi} A_{nm} \psi N_{z,m} \ , \tag{A2}$$

where h is Planck's constant, ψ the spectral line shape satisfying $\int \psi \, d\nu = 1$, and A_{nm} the Einstein coefficient defined by

$$A_{nm} = \frac{8\pi^2 e^2}{m_e c^3} \nu^2 \frac{g_n}{g_m} f_{mn} \ . \tag{A3}$$

Here, m_e and e are the mass and the charge of electrons, c is the speed of light, g the statistical weight, and f_{mn} the absorption oscillator strength.

By detailed balance, κ_ν is given by

$$\kappa_\nu = \frac{\pi e^2}{m_e c} f_{mn} \psi N_{z,n} \ , \tag{A4}$$

and

$$\kappa'_\nu = \kappa_\nu \left[1 - \frac{g_n}{g_m} \frac{N_{z,m}}{N_{z,n}} \right] . \tag{A4'}$$

An electron in the bound level m is excited up to the level n by this photoabsorption process. In Eq. (1), this effect is explicitly written in the form

$$\frac{dN_{z,n}}{dt} = \cdots - \sum_{n<k} X_{z,kn} N_{z,n} + \sum_{m<n} X_{z,nm} N_{z,m} \ , \tag{A5}$$

where

$$X_{z,nm} N_{z,m} = \frac{4\pi}{h\nu} \int \kappa'_\nu I_\nu \, d\nu \ . \tag{A6}$$

Here, the integration is done over the spectral shape ψ of the line.

In the HAM, this photoexcitation should be incorporated with the average-ion model—Eq. (2). It is clear from the discussion in the Sec. V that photoexcitation only of the average ion is not enough and that various ions should be taken into account. For this purpose, we propose to use a z-averaged photoexcitation X_{mn}, defined to be

$$X_{mn} \equiv \sum_z X_{z,nm} \frac{N_z}{N_i} \ , \tag{A7}$$

in Eq. (2) as follows:

$$\frac{d(NP_n)}{dt} = \cdots - \sum_{n<k} X_{kn} P_n Q_k + \sum_{m<n} X_{nm} P_m Q_n \ . \tag{A8}$$

APPENDIX B

The average ion model treats multiply charged ions as a groups of "ions" having an average charge z. To obtain the properties of average ions the number of electrons in different atomic levels is needed. This is determined by averaging the number of electrons in a particular level of all the ions grouped to the average ion. In Eq. (1) $N_{z,n}$ is the number of ions with charge z and one electron excited to the nth level, other electrons being in ground-state levels. Let the number of electrons in the kth level of a "real ion" ($N_{z,n}$) be denoted by $\xi_{k;z,n}$. Since it is assumed that only one electron is excited in the nth level, $\xi_{k;z,n} = 1$ for $k = n$, further $\xi_{k;z,n} \neq 0$ for k representing levels of ground state (denoted in the following as g), and $\xi_{k;z,n} = 0$ for other values of k.

Multiplying Eq. (1) with $\xi_{k;z,n}$ and summing over different charge state z and levels n, we obtain

$$\sum_{z,n} \xi_{k;z,n} \frac{dN_{z,n}}{dt} = - \sum_{z,n,m} I_{z,n;z+1,m} \xi_{k;z,n} N_{z,n} N_e + \sum_{z,m',n} I_{z,m';z+1,n} \xi_{k;z+1,n} N_{z,m'} N_e + (R,E,D) \ . \tag{B1}$$

To simplify, only ionization terms are written explicitly. Other terms of Eq. (1) have a similar form and are represented symbolically by (R,E,D).

The electron population is defined as

$$P_k N \equiv \sum_{z,n} \xi_{k;z,n} N_{z,n} \ . \tag{B2}$$

Now the rate equation for the population in a level k can be distinguished in two different cases: (1) k is not a ground-state level and (2) k is a ground-state level.

(1) $k \neq g$. In this case $\xi_{k;z,n}=1$ for $k=n$ and $\xi_{k,z,n}=0$ for $k \neq n$. Equation (B1) for this case can be written as

$$\frac{dP_k N}{dt} = -\sum_{z,m} I_{z,k;z+1,m} N_{z,k} N_e + \sum_{z,m'} I_{z,m';z+1,k} N_{z,m'} N_e + (R,E,D) \ . \tag{B3}$$

It should be noted that in the term $I_{z,k;z+1,m}$ in Eq. (B3) m should be a ground-state level if the kth electron is ionized, while m should be equal to k if the other electron is ionized. Therefore, it is evident that $m=k=n$ or $m=g$, and $m'=k=n$ and Eq. (B3) leads to

$$\frac{dP_k N}{dt} = -\sum_{z} I_{z,k;z+1,g} N_{z,k} N_e + (R,E,D) \ . \tag{B3'}$$

(2) $k=g$. In this case $m=n$ or g and $n=m'$ or g. Equation (B1) now reads

$$\frac{dP_k N}{dt} = -\sum_{z,n} I_{z,n;z+1,n} \xi_{k;z,n} N_{z,n} N_e - \sum_{z,n\neq g} I_{z,n;z+1,g} \xi_{k;z,n} N_{z,n} N_e + \sum_{z,m'} I_{z,m';z+1,m'} \xi_{k;z+1,m'} N_{z,m'} N_e + \sum_{z,m'\neq g} I_{z,m';z+1,g} \xi_{k;z+1,g} N_{z,m'} N_e + (R,E,D) \ . \tag{B4}$$

In this case, $\xi_{k;z,n}=\xi_{k;z+1,g}$ for $n \neq g$ because the number of electrons in the ground level is z_0-z-1 in both terms; it is z_0-z-1 (1 is due to the excited electron) for $\xi_{k;z,n}$ and $z_0-(z+1)$ for $\xi_{k;z+1,g}$. In contrast, $\xi_{k;z,n} - \xi_{k;z+1,g}=1$ for $n=g$. Therefore, the second and the fourth terms cancel each other and Eq. (B4) reduces to

$$\frac{dP_k N}{dt} = -\sum_{z,n} I_{z,n;z+1,n} N_{z,n} N_e + (R,E,D) \ , \tag{B4'}$$

where $\xi_{k;z,n} - \xi_{k;z+1,n}=1$ is used.

Since $I_{z,k;z+1,g}$ and $I_{z,n;z+1,n}$ implicitly include the number of electrons in the ionizing shell,[12] which is ξ_k ($=\xi_{k;z,k}$ or $\xi_{k;z,n}$), it is appropriate to introduce [see Eq. (9)] $I_{z,k} \equiv I_{z,k;z+1,g}/\xi_{k;z,k}$ and $I_{z,n;z+1,n}/\xi_{k;z,n}$. Accordingly, both Eqs.(B3') and (B4') lead to

$$\frac{dP_k N}{dt} = -\sum_{z,n} I_{z,n} \xi_k N_{z,n} N_e + (R,E,D) \ , \tag{B5}$$

for all k; note that for $k \neq g$ [Eq. (B3')] only the term $k=n$ in Eq. (B5) remains because $\xi_{k;z,n}=0$ for $k \neq n$.

If the distribution of z sharply peaks at $z=z^a$ and $I_{z,k}$ for the neighboring ions can be approximated by $I_{z^a,k}$, Eq. (B5) reduces to

$$\frac{dP_k N}{dt} = -I_{z^a,k} P_k N N_e + (R,E,D) \ , \tag{B6}$$

by use of Eq. (B2). This is the equation for the average ion.

[1] D. G. Colombant, K. G. Whitney, D. A. Tidman, N. K. Winsor, and J. Davis, Phys. Fluids **18**, 1687 (1975).
[2] D. Duston and J. Davis, Phys. Rev. A **21**, 1664 (1980).
[3] S. Chandrasekhar, *An Introduction to the Study of Stellar Structure* (Dover, New York, 1939).
[4] B. F. Rozsnyai, Phys. Rev. A **5**, 1137 (1972).
[5] W. A. Lokke and W. H. Grasberger, Lawrence Livermore Laboratory Report No. UCRL-52276, 1977 (unpublished).
[6] D. E. Post, R. V. Jensen, C. B. Tarter, W. H. Grasberger, and W. A. Lokke, At. Data Nucl. Data Tables **20**, 397 (1977).
[7] R. M. More, Lawrence Livermore National Laboratory Report No. UCRL-84991, 1981 (unpublished).
[8] S. Kiyokawa, T. Yabe, and T. Mochizuki, Jpn. J. Appl. Phys. **22**, L772 (1983).
[9] D. Salzmann and A. Krumbein, J. Appl. Phys. **49**, 3229 (1978).
[10] M. Busquet, Phys. Rev. A **25**, 2302 (1982).
[11] H. Mayer, Los Alamos Scientific Laboratory Report No. LA647, 1947 (unpublished).
[12] R. K. Landshoff and J. D. Perez, Phys. Rev. A **13**, 1619 (1976).
[13] W. Lotz, Z. Phys. **216**, 241 (1968).
[14] M. J. Seaton, in *Atomic and Molecular Processes,* edited by D. R. Bates (Academic, New York, 1962), p. 375.
[15] R. W. P. McWhirter, in *Plasma Diagnostic Techniques,* edited by R. H. Huddlestone and S. L. Leonard (Academic, New York, 1965).
[16] H. Griem, Plasma Spectroscopy (McGraw-Hill, New York, 1964), p. 161.
[17] A. Burgess, Astrophys. J. **141**, 1588 (1965).
[18] O. Bely, Proc. Phys. Soc. London **88**, 587 (1966).
[19] M. Blaha, Astrophys. J. **157**, 473 (1969).
[20] S. Kiyokawa, T. Yabe, N. Miyanaga, K. Okada, H. Hasegawa, T. Mochizuki, T. Yamanaka, C. Yamanaka, and T. Kagawa, Phys. Rev. Lett. **54**, 1999 (1985).
[21] A. H. Gabriel and C. Jordan, *Case Studies in Atomic Collision Physics 2,* edited by E. W. McDaniel and M. R. C. McDowell (North-Holland, Amsterdam, 1972), p. 211.